Electrogenerated chemiluminescence of Si quantum dots in neutral aqueous solution and its biosensing application

Yong-Ping Dong, Jiao Wang, Ying Peng, Jun-Jie Zhu

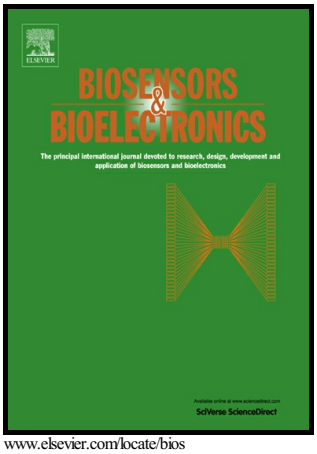

www.elsevier.com/locate/bios

PII: S0956-5663(16)31006-5
DOI: http://dx.doi.org/10.1016/j.bios.2016.10.011
Reference: BIOS9233

To appear in: *Biosensors and Bioelectronic*

Received date: 19 August 2016
Revised date: 2 October 2016
Accepted date: 3 October 2016

Cite this article as: Yong-Ping Dong, Jiao Wang, Ying Peng and Jun-Jie Zhu, Electrogenerated chemiluminescence of Si quantum dots in neutral aqueou solution and its biosensing application, *Biosensors and Bioelectronic* http://dx.doi.org/10.1016/j.bios.2016.10.011

Electrogenerated chemiluminescence of Si quantum dots in neutral aqueous solution and its biosensing application

Yong-Ping Dong[a], Jiao Wang[a,b], Ying Peng[a], Jun-Jie Zhu[b*]

[a]School of Chemistry and Chemical Engineering, Anhui University of Technology, Maanshan 243002, China

[b]State Key Laboratory of Analytical Chemistry for Life Science, School of Chemistry and Chemical Engineering, Nanjing University, Nanjing 210093, China

[*]Corresponding author. Tel&fax: +86-25-83597204. jjzhu@nju.edu.cn

Abstract

Electrogenerated chemiluminescence (ECL) of semiconductor quantum dots (QDs) has been considered as a powerful technique in the fabrication of biosensor, however, high-toxicity of heavy metal ion containing in QDs severely limits their further applications, and the search for the alternative benign nanomaterials with high ECL efficiency is urgent. Herein, ECL behavior of eco-friendly silicon quantum dots (SiQDs) was reported in neutral aqueous condition. Stable and intense cathodic ECL emission was obtained in phosphate buffer solution (PBS) with $K_2S_2O_8$ as coreactant. ECL resonance energy transfer (ECL-RET) system was established with SiQDs ECL as energy donor and gold nanoparticles (AuNPs) as energy acceptor, based on which

a novel ECL biosensor was fabricated. AuNPs was connected at the terminal of hairpin DNA to form a signal probe. When the probe was modified on SiQDs, ECL-RET occurred due to the short distance between AuNPs and SiQDs, resulting in the apparent decrease of ECL signal. Target DNA can open the loop of hairpin DNA, and move AuNPs away from the electrode surface. As a result, the ECL-RET process was hampered, and the ECL emission resumed. The increased ECL signals varied linearly with the target DNA concentrations in the range of 0.1 fM to 1 pM with the detection limit of 0.016 fM (3σ). The proposed ECL sensor exhibited highly sensitivity and good selectivity in the detection of target DNA.

Keywords: Electrogenerated chemiluminescence; Si quantum dots; Resonance energy transfer; DNA; Biosensor

1. Introduction

It is well-known that the quantum confinement of excitons in semiconductor quantum dots (QDs) leads to excellent optical properties that can be exploited in bioconjugates and optical biosensing (Bruchez et al., 1998; Ding et al., 2003; Sapsford et al., 2004; Wang et al., 2002). In the past few decades, electrogenerated chemiluminescence (ECL) of semiconductor QDs, including CdS, CdSe, CdTe and their composites, has become a very powerful analytical technique owing to the advantages, such as good stability, simplified optical setup, low cost, and low background noise (Miao et al., 2008; Richter et al., 2004). Although the semiconductor QDs have already been accepted as ECL indicator for their effective and valuable ECL behaviors, heavy metals as the essential elements in these QDs have raised serious health and environmental

concerns (Derfus et al., 2004). Therefore, searching for alternative nanomaterials of semiconductor QDs with good ECL activities has become an urgent challenge.

To maintain a benign environment, low-toxicity silicon and carbon nanostructures are preferred in many fields. In contrast with common semiconductor QDs, luminescent carbon group QDs not only exhibit many fascinating optical properties, but also present some additional advantages over the heavy metal containing semiconductor QDs, such as chemical inertness, good stability, biocompatibility, low toxicity, easy preparation, and environmental friendliness (Ding et al., 2002; Sham et al., 1993; Sun et al., 2006; Wilson et al., 1993). Silicon and carbon QDs have been considered as highly promising nanomaterials for biological and biomedical application (Baker et al., 2010; Zheng et al., 2009; Lu et al., 2012; Liu et al., 2012; Michalet et al., 2005; Song et al., 2010; He et al., 2010). During the past few years, many exciting results were obtained in the development of SiQDs based fluorescent biological probes. For example, hydrophilic molecule capped, polymer coated, and micelle encapsulated SiQDs have been prepared for biological imaging (Li et al., 2004; Warner et al., 2005; Erogbogbo et al., 2008, 2011; He et al., 2009a, 2009b; Shiohara et al., 2010). In 2002, ECL of SiQDs was firstly reported by Bard et al. in nonaqueous condition (Ding et al., 2002). Since then, QDs ECL was widely investigated and many novel biosensors based on QDs ECL were proposed (Li et al., 2012). However, up to date, SiQDs ECL has not been reported in aqueous condition because SiQDs often suffered from poor aqueous dispersibility due to surface-covered hydrophobic functional groups. Recently, intensive research has been done in producing hydrophilic SiQDs to make the resultant SiQDs water dispersible and suitable for biological applications (Erogbogbo et al., 2008; Montalti et al., 2015; He et al., 2009, 2011; Zhong et al., 2013). The successful synthesis of

water dispersible SiQDs makes it possible to explore SiQDs ECL in aqueous condition as well as its biosensing application.

Resonance energy transfer (RET) is a powerful technique for probing changes in the distance between donors and acceptors. Various RET systems have been developed for bioassays (Carriba et al., 2008; Lee et al., 2012; Wang et al., 2014; Shi et al., 2006; Clapp et al., 2004; Hou et al., 2014; Li et al., 2008). Among them, ECL-RET has been considered as a promising approach for further study of energy transfer due to the advantage of the absence of background light emission, high sensitivity, wide dynamic range, and so on. The ECL-RET techniques have been used for DNA detection, cytosensing, and immunoassay (Shan et al., 2009; Zhou et al., 2012; Wu et al., 2011, 2012; Tian et al., 2012). However, the inherent toxicity of semiconductor QDs used in most ECL-RET systems may raise serious health and environmental problems. Therefore, the search for benign nanomaterials with strong and stable ECL emission as donor has become an urgent challenge.

Herein, water dispersible SiQDs were prepared via in situ growth under microwave irradiation using 3-aminopropyl trimethoxysilane as the silicon source according to the reported method (Zhong et al., 2013). The as-prepared SiQDs could generate strong cathodic ECL with $K_2S_2O_8$ as coreactant in neutral aqueous condition. ECL-RET could occur between SiQDs ECL and gold nanoparticles, based on which an ECL biosensor was fabricated and used in the sensitive and selective detection of target DNA.

2. Experimental

2.1. Materials

Tris(2-carboxyethyl)phosphine (TCEP) and mercaptoacetic acid (MCH) were obtained from Sigma-Aldrich. 3-aminopropyl trimethoxysilane and poly-(diallyldimethylammonium chloride) (PDDA, 20%, w/w in water, MW = 200000–350000) were purchased from Aladdin Chemistry Co., Ltd. Chloroauric acid ($HAuCl_4 \cdot 4H_2O$) was purchased from Shanghai Reagent Company. Trisodium citrate and potassium persulfate were obtained from Nanjing Chemical Reagent Co., Ltd. All other chemicals were of analytical reagent grade, and double distilled water was used throughout. 0.1 mol L^{-1} pH 7.4 phosphate buffer solution (PBS) was used to prepare the working solution.

The DNA used in this work was synthesized and purified by Shanghai Sangon Biological Engineering Technology & Service Co., Ltd. The target DNA is complementary to the loop of hairpin DNA, which will cause the hairpin DNA to adopt the open form. The DNA sequences used are as follows (The italicized part is the complementary strand of the target DNA):

Hairpin DNA: 5′-NH_2-$(CH_2)_6$-GGA AGT ***CTC AGC AAG CTT TAA CTC*** ACT TCC-$(CH_2)_6$-SH-3′

Target DNA: 5′-GAG TTA AAG CTT GCT GAG-3′

1-base mismatched DNA: 5′-GAG TT***G*** AAG CCT GCT GAG-3′

3-base mismatched DNA: 5′-GAG TT***G*** AAG C***G***T GCT G***T***G-3′

Random DNA: 5′-TTT AGA GGT GTT AAG CCA-3′

2.2. Synthesis of AuNPs

5-nm diameter gold nanoparticles were synthesized according to the literature with minor modification (Brown et al., 2000). 2.54 mL of 10 mM $HAuCl_4$ was added into 88 mL double-distilled water. When the solution was heated to boil, 2 mL of 38.8 mM trisodium citrate was

added into the mixture solution under vigorously stirring. Then, 1 mL of 0.075% $NaBH_4$ was added and stirred at the boiling point for 15 min, during which time a color change from gray to blue to purple was observed. The colloid was stored in the refrigerator for further use. The synthesized AuNPs was characterized by TEM and UV-vis absorption spectroscopy (Fig. S1 and S2). The results revealed that well-dispersed gold nanoparticles were obtained.

2.3. Synthesis of SiQDs

The SiQDs precursor solution was prepared according to the literature with minor revision (Zhong et al., 2013). 3 mL of 3-aminopropyl trimethoxysilane was added into 12 mL N_2-saturated aqueous solution containing 0.632 g trisodium citrate. After 15 min of stirring, the precursor solution was transferred into a microwave reactor. The SiQDs was prepared under 160 °C for 15 min. After microwave irradiation, the SiQDs sample was removed after the temperature naturally decreased to lower than 30 ^{o}C. The residual impurities were removed by dialysis (1 kDa). The obtained SiQDs were characterized by HRTEM, FT-IR, FL, and UV-vis absorption spectroscopy.

2.4. Preparation of AuNPs/hairpin DNA Probe

10 μL of 1 μM hairpin DNA was activated with 0.15 μL of 10 mM TCEP in 0.01 mol L^{-1} PBS containing 0.1 mol L^{-1} NaCl for 1 h to open the disulfide bond. Then, 100 μL of AuNPs was added into the mixture solution and incubated at 25 ^{o}C for 30 min. Finally, 10 μL of 10 mM of MCH was added and incubated for 2 h to prevent the unspecific adsorption of AuNPs. The mixture was kept at 4 ºC for further use.

2.5. Fabrication of ECL biosensor

A glassy carbon electrode (GCE, 3 mm in diameter) was polished with 0.3 and 0.05 μm Al_2O_3 power, and cleaned in an ultrasonic cleaner with alcohol and double-distilled water sequentially. The cleaned electrode was dried by nitrogen. Then, 10 μL of SiQDs was spread on a cleaned bare GCE to form SiQDs modified electrode (denoted as SiQDs/GCE). After the film was dried in the dryer, the electrode was soaked in 1% PDDA solution for 1 h at room temperature. After drying, 10 μL of AuNPs/hairpin DNA probe solution was dropped onto its surface to incubate at 37 °C for 1 h (denoted as AuNP/hairpin/SiQDs/GCE). For comparison, the probe without AuNPs was used to form hairpin/SiQDs/GCE. The electrode was washed by 10 mM PBS to remove the unstable probe on surface. The resulted electrode was incubated with target DNA of different concentrations for 2 h at 37 °C (tDNA/AuNPs/hairpin/SiQDs/GCE).

3. Results and discussion

3.1. Characterization of SiQDs

The synthesized SiQDs were characterized by HRTEM, FT-IR, FL, and UV-vis absorption spectroscopy, respectively. It can be found from Fig.1A that the resultant SiQDs appears as spherical particles with good monodispersity. The inset of Fig.1A shows the well-resolved (220) lattice planes of 0.19 nm spacing, demonstrating the excellent crystallinity of SiQDs (Zhong et al., 2013). The size distribution in Fig.1B shows that SiQDs have an average size of 6.72 nm by measuring more than 400 particles. The FT-IR spectrum of SiQDs was shown in Fig.1C. The absorption peak at 3350 cm^{-1} can be assigned as the O-H stretching vibration. The C-H bond stretching vibrations can be found at 2930 cm^{-1}. The characteristic C=C stretching vibration appears at 1590 cm^{-1}. The typical Si-O-Si asymmetric stretching peak is located at 1120 cm^{-1} and the C-Si stretching peak is located at 694 cm^{-1} (Jiang et al., 2016). Fig.1D shows UV-FL spectra

of the resultant SiQDs. The results revealed that SiQDs possess good optical properties with wide absorbance peak and symmetrical FL peak located at 465 nm.

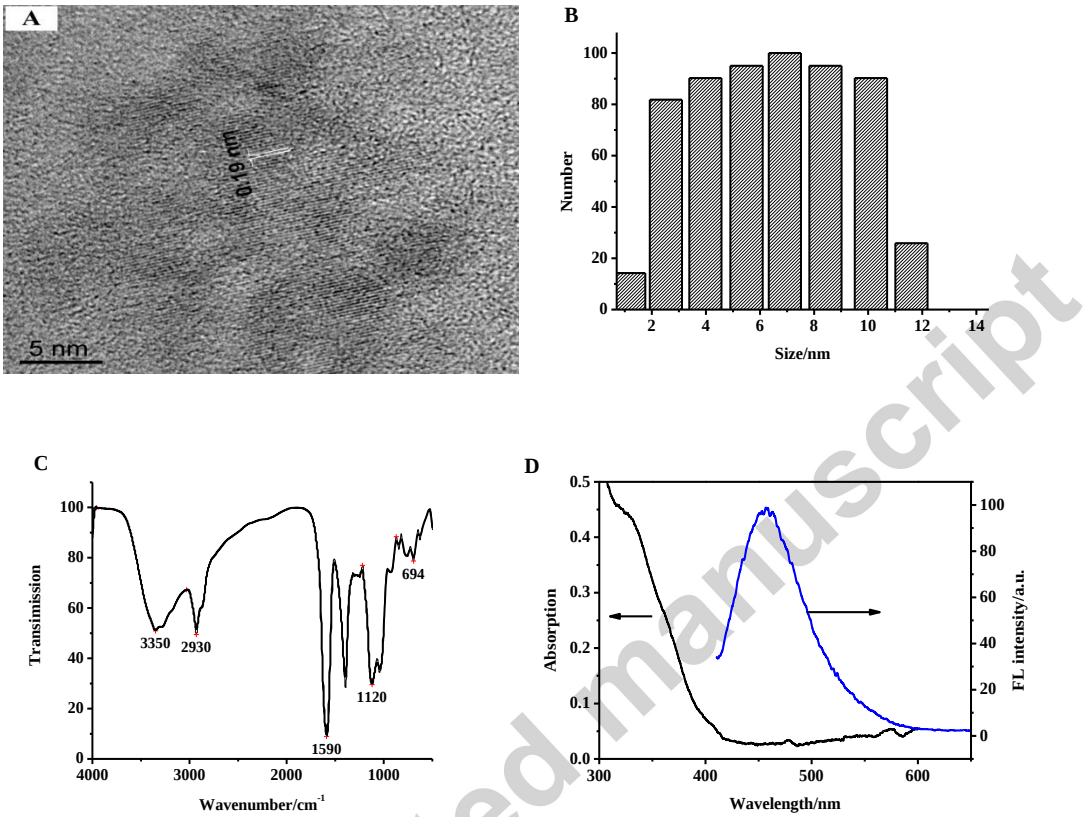

Fig.1. (A) HRTEM image of SiQDs, (B) Size distribution of SiQDs, (C) FT-IR spectrum of SiQDs, (D) Fluorescence and UV-vis absorption spectra of SiQDs.

3.2. Electrochemistry and ECL of SiQDs

ECL of SiQDs/GCE was investigated in neutral phosphate buffer solution (PBS) with $K_2S_2O_8$ as coreactant. Fig. 2A shows that weak ECL can be obtained at the bare GCE in PBS containing $K_2S_2O_8$, which can be assigned to the background light emission. When the SiQDs/GCE was studied in PBS without $K_2S_2O_8$, no light emission was observed, revealing that SiQDs can not generate ECL without coreactant. Strong cathodic ECL was observed when the SiQDs/GCE was studied in PBS containing $K_2S_2O_8$, and the intensity of ECL increased nearly 16-times compared

with that of the bare GCE. The inset of Fig. 2A displays the ECL intensities of the SiQDs/GCE under 11 repeated cyclic voltammetric scans. It can be found that the cathodic ECL intensity from SiQDs is quite stable with a relative standard deviation of 3.6 %. The strong and stable ECL emission in neutral aqueous condition revealed that SiQDs have good application potential in bioassay field.

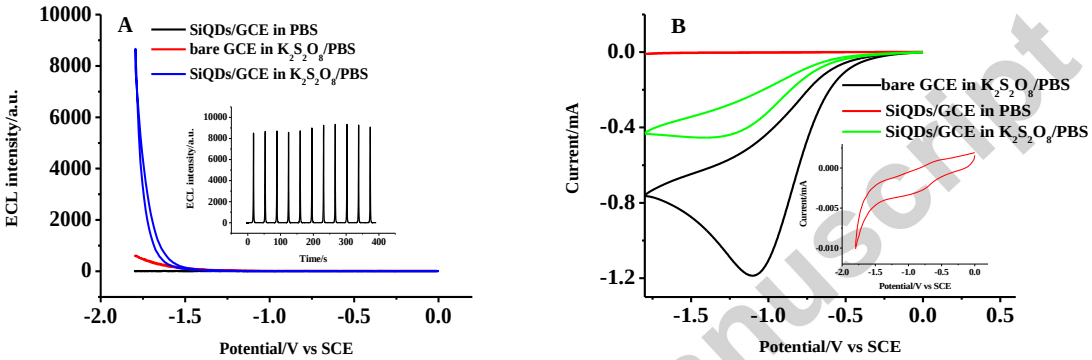

Fig.2. (A) ECL curves of the bare GCE and the SiQDs/GCE in pH 7.4 0.1 mol L^{-1} PBS in the absence and presence of $K_2S_2O_8$. The inset is ECL emission of the SiQDs/GCE under continuous cyclic voltammetry for 11 cycles. (B) Cyclic voltammograms of the bare GCE and the SiQDs/GCE in pH 7.4 0.1 mol L^{-1} PBS in the presence and absence of $K_2S_2O_8$. The inset is the enlarged CV curves of SiQDs/GCE in PBS. Scan rate, 100 mV s^{-1}; $K_2S_2O_8$, 0.1 mol L^{-1}.

Electrochemical behaviors of the SiQDs/GCE were studied and shown in Fig. 2B. One broad and strong reduction peak located -1.10V (vs SCE) at the bare GCE in $K_2S_2O_8$/PBS mixing solution can be assigned to the reduction of $K_2S_2O_8$. As shown in the inset of Fig. 2B, SiQDs can be reduced at -0.75 V. Extremely weak reduction peak suggests that electrochemical activity of SiQDs is poor. The apparent decrease of the reduction peak of $K_2S_2O_8$ at the SiQDs/GCE suggests that the reduction products of SiQDs can react with $K_2S_2O_8$, which should be responsible for the generation of strong ECL emission.

3.3. Impact factors of ECL emission

Electrochemical impedance spectroscopy and several impacting factors of ECL (the amount of SiQDs, the concentration of $K_2S_2O_8$, and the pH value) were investigated (Fig. S3). The results reveal that ECL intensities increased with the increase of the modified SiQDs, indicating that SiQDs is involved in ECL emission. Electrochemical impedance spectroscopy reveals that the charge transfer resistance increased with the increase of SiQDs amount, which is due to the poor conductivity of SiQDs as well as the electrostatic repulsive force between negatively charged SiQDs and $[Fe(CN)_6]^{3-/4-}$ probe. The EIS results suggest that strong cathodic ECL should be result from the reaction between SiQDs and $K_2S_2O_8$ but not from the electrocatalytical effect of nanoparticles. ECL signals increase with the increase of $K_2S_2O_8$ concentration, suggesting that $K_2S_2O_8$ participate ECL reactions. ECL signals increase with the increase of pH values from 6.0 to 7.0, and reach a plateau at neutral condition. Further increase of pH, ECL signals begin to decrease. The intense ECL obtained in neutral condition reveals that the present ECL system is suitable for the fabrication of biosensor.

3.4. ECL mechanism

In order to elucidate the mechanism of the cathodic ECL emission, the FL and UV-vis absorption spectra of SiQDs and $K_2S_2O_8$ mixture were recorded (Fig. S4). The UV-vis absorption spectrum of SiQDs/$K_2S_2O_8$ mixture is the simple overlap of SiQDs and $K_2S_2O_8$ absorption spectra, revealing that SiQDs can not react with $K_2S_2O_8$ under the ground state. However, the FL of the SiQDs/$K_2S_2O_8$ mixture decreased significantly compared with the pure SiQDs, revealing that $K_2S_2O_8$ could react with the excited state of SiQDs and lead to the decrease of FL intensity.

The maximum cathodic ECL emission located at 475 nm which is almost the same as the FL spectrum of SiQDs, revealing that the light emitter of the cathodic ECL is the excited state of SiQDs (Fig. S5). Electrochemical results supported that the reduction products of SiQDs can react with $K_2S_2O_8$. Therefore, the ECL mechanisms can be proposed according to the literature and the experimental results as follows (Zheng et al., 2009; Dong et al., 2010).

$$SiQDs + e \rightarrow SiQDs^{\bullet} \quad (1)$$

$$SiQDs^{\bullet} + S_2O_8^{2-} \rightarrow S_2O_8^{2-\bullet} + SiQDs \quad (2)$$

$$S_2O_8^{2-} + e \rightarrow S_2O_8^{2-\bullet} \quad (3)$$

$$S_2O_8^{2-\bullet} \rightarrow SO_4^{2-} + SO_4^{-\bullet} \quad (4)$$

$$SiQDs^{\bullet} + SO_4^{-\bullet} \rightarrow SiQDs^{*} + SO_4^{2-} \quad (5)$$

$$SiQDs^{*} \rightarrow SiQDs + h\nu \quad (6)$$

3.5. Fabrication of ECL biosensor

Gold nanoparticles were often used in fabrication of biosensor due to its catalytical effect and biocompatibility (Pingarron et al., 2008; Shen et al., 2012). Previous work revealed that gold nanoparticles could quench light emission due to the energy transfer (Jennings et al., 2006). It was found in the present work that the surface plasmon absorption peak of AuNPs is overlapped with the FL of SiQDs, revealing that it is possible to establish energy donor/acceptor pair involving SiQDs and AuNPs (Fig. S2). When AuNPs were added in SiQDs solution, FL intensity of SiQDs decreased apparently, revealing that FL resonance energy transfer can occur between SiQDs and AuNPs (Fig. S6). It was also found that the cathodic ECL signal decreased in the presence of AuNPs, suggesting that ECL resonance energy transfer (ECL-RET) between

SiQDs and AuNPs is possible. Previous work revealed that ECL-RET efficiency is highly dependent on the extent of spectral overlap and the distance between energy donor and acceptor (Sapsford et al., 2006). Therefore, in the present work, the distance between SiQDs and AuNPs was adjusted by using the complementary interaction between the hairpin DNA and the target DNA, which could modulate the ECL-RET efficiency, and ECL intensity varied accordingly.

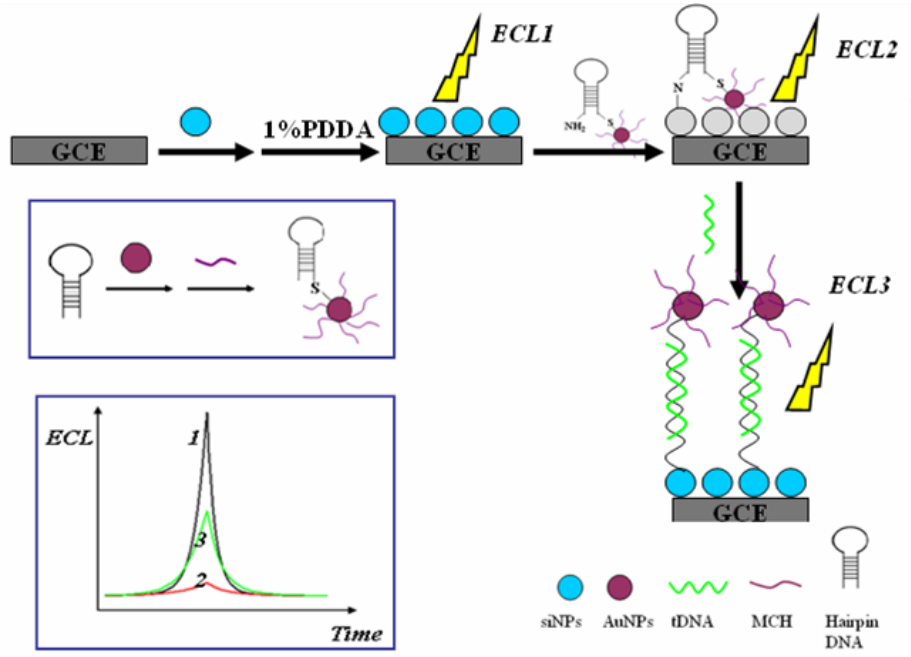

Fig.3. Schematic representation of the fabrication of ECL biosensor and the detection of target DNA

The protocol for the fabrication of ECL biosensor was shown in Fig.3. Firstly, SiQDs were immobilized on a bare GCE to generate strong ECL in the presence of $K_2S_2O_8$. PDDA was cast on SiQDs film to strength the stability of SiQDs/GCE and facilitate the immobilization of hairpin DNA. Then, gold nanoparticles modified hairpin DNA was connected at the modified electrode surface (AuNPs/hairpin/SiQDs/GCE) through the interaction between -NH_2 groups of hairpin DNA and -COOH groups of SiQDs, which can form energy transfer donor/acceptor pair with

SiQDs and result in the decrease of ECL signal. Finally, the hairpin DNA was hybridized with the target DNA (tDNA/AuNPs/hairpin/SiQDs/GCE), which can move AuNPs away from the electrode surface and recover ECL emission. The variation of ECL signals is related to the target DNA concentrations, and can be used in the sensitive detection of target DNA.

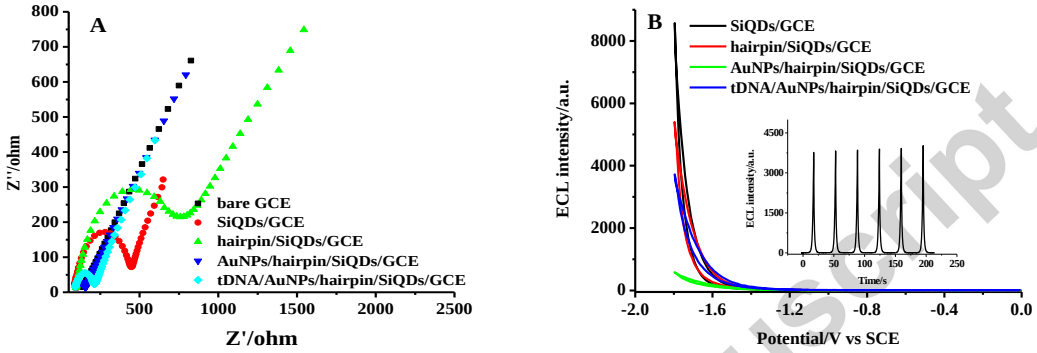

Fig.4. (A) Nyquist diagram of electrochemical impedance spectra recorded from 0.01 to 10^5 Hz for $[Fe(CN)_6]^{3-/4-}$ (10 mM, 1:1) in 0.1 mol L^{-1} pH 7.4 PBS containing 0.1 mol L^{-1} KCl. (B) ECL profiles of different processes of the fabrication of biosensor. The inset is ECL emission from the biosensor after incubating in 50 fM target DNA solution under continuous cyclic voltammetry for 6 cycles. PBS, 0.1 mol L^{-1}; pH, 7.4; scan rate, 100 mV s^{-1}.

Electrochemical impedance spectroscopy (EIS) was used to characterize the fabrication process of the ECL biosensor. It can be found from Fig. 4A that the impedance spectra of the modified electrodes consisted of a semicircle at high AC frequency and a line at low AC frequency, suggesting that the electrode process was controlled by charge transfer at high frequency and by diffusion at low frequency. Because the diameter of semicircle equals the charge transfer resistance (R_{ct}), the variation of the diameter can be used to reflect the restricted diffusion of the redox probe through the multilayer modified on the GCE. When SiQDs were modified on the bare GCE, R_{ct} increased greatly due to the poor conductivity of SiQDs and

electrostatic repulsive force between the negatively charged SiQDs and the probe. When hairpin DNA was modified on the SiQDs film, R_{ct} increased significantly due to the negatively charged and the insulating property of DNA (Fig. S7). R_{ct} decreased to the level of the bare GCE when AuNPs was connected on the terminal of hairpin DNA, suggesting that good conductivity of AuNPs is facile for charge transfer through the modified film. When hairpin DNA was hybridized with target DNA, the loop of hairpin DNA was opened and AuNPs was moved away from the electrode surface. As a result, R_{ct} increased again. The EIS results can support the successful stepwise fabrication of the ECL biosensor.

The ECL responses of the modified electrodes under different stages were recorded as shown in Fig. 4B. Strong cathodic ECL can be obtained at the SiQDs/GCE. When hairpin DNA was modified on the SiQDs film, the intensity of ECL decreased due to the poor conductivity of DNA, which could hinder the charge transfer through the electrode surface. When AuNPs were connected on the terminal of hairpin DNA, the distance between AuNPs and SiQDs is near enough for the energy transfer (Shan et al., 2009). As a result, SiQDs can transfer its ECL energy to AuNPs, leading the decreased ECL signal. When hairpin DNA was hybridized with target DNA, the loop structure was opened and AuNPs was released from the electrode surface. The long distance between SiQDs and AuNPs destroyed the energy transfer process. As a result, the ECL signal recovered. The variation of ECL intensities can be indirectly used in the sensitive detection of the target DNA. The inset of Fig. 4B displays the ECL emission of the biosensor after it was incubated in 50 fM target DNA solution under continuous potential scan. The stable ECL signals suggested that the biosensor is suitable for DNA detection.

3.6. Analytical performance of the biosensor

In order to evaluate the quantitative behavior of the proposed ECL biosensor for the target DNA, the ECL intensity was measured upon the target DNA concentration. After the biosensor was incubated in different concentrations of the target DNA, the ECL intensities were recorded as shown in Fig. 5A. It can be found that the ECL intensity increased gradually with the increase of target DNA concentration. The calibration curve revealed a good linear relationship between the ECL intensity and the logarithm of DNA concentration in the range from 0.1 fM to 1 pM with the correlation coefficient of 0.994 as shown in the inset of Fig.5A. The detection limit of the ECL sensor was determined at levels down to 0.016 fM (3σ, n=6). The comparison of the various ECL sensors for DNA was listed in Table S1. It can be found that the sensitivity of the present ECL biosensor is superior to most of other reported biosensors. The reproducibility of the proposed biosensor for target DNA was evaluated from the response to 50 fM DNA at six different electrodes. The relative standard derivation (RSD) was 3.5%, demonstrating that the biosensor possessed acceptable reproducibility. When the biosensor was stored in pH 7.4 PBS at 4 ^{o}C for 10 days, the ECL signal retained 95.4% of the original ECL response, indicating a good stability of the biosensor.

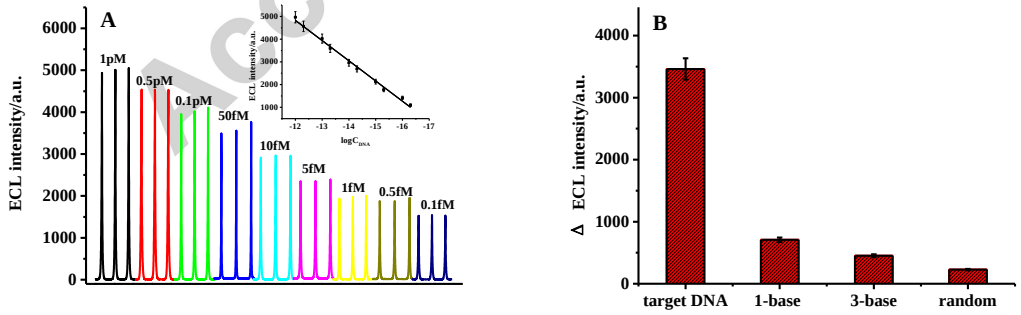

Fig.5. (A) The ECL signals of the biosensor incubated in different concentrations of target DNA. The inset is the corresponding logarithmic calibration curve. (B) Comparison of the ECL intensity changes for the sensors hybridized with target DNA, one-base mismatched target DNA,

three-base mismatched target DNA, and random sequence DNA in the same concentration (100 fM).

3.7. Specificity of the ECL biosensor

In order to investigate the specific response of the ECL biosensor to the target DNA, control experiments were performed by incubating the ECL biosensor in four aqueous solutions containing target DNA, single-base mismatched target DNA, three-base mismatched target DNA, and random sequence DNA, respectively. Fig. 5B shows the comparison of the ECL intensity changes of the ECL biosensors for the same concentration of different DNA. The significant ECL signal change was observed after the ECL biosensor was incubated in the target DNA because the loop of hairpin DNA can be completely opened by the target DNA. The ECL signal change for the random sequence DNA was only 5.5% of that for complementary target DNA, attributed to the fact that the loop of hairpin DNA cannot be entirely opened. The response to the one-base mismatched target DNA and the three-base mismatched target DNA was only 20% and 13% of that for complementary target DNA. The comparison indicated that this method had high sequence specificity, and this detection approach had potential application in single nucleotide analysis.

4. Conclusion

Strong cathodic ECL of SiQDs was obtained in neutral aqueous solution with $K_2S_2O_8$ as coreactant. ECL resonance energy transfer can occur between SiQDs ECL and gold nanoparticles, resulting in the decreased ECL emission. An ECL biosensor was proposed based on the ECL-RET process and can be used in the sensitive detection of target DNA. In the range of 0.1 fM to 1 pM, the ECL intensity changed linearly with the logarithm of DNA concentration

with the detection limit of 0.016 fM. As SiQDs is eco-friendly compared with semiconductor QDs, the application of SiQDs ECL in the fabrication of biosensor will provide a new avenue for the biosensing application of ECL techniques.

Acknowledgments

This research was supported by National Natural Science Foundation of China (Nos 21335004, 21427807, 21575002), Natural Science Foundation of Anhui Province (No. 1408085MF114), Natural Science Foundation from the Bureau of Education of Anhui Province (No. KJ2015A075).

References

Baker, S.N., Baker, G.A., 2010. Angew. Chem., Int. Ed. 49, 6726-6744.

Bruchez, M., Moronne, M., Gin, P., Weiss, S., Alivisatos, A.P., 1998. Science 281, 2013-2016.

Brown, K.R., Walter, D.G., Natan, M.J., 2000. Chem. Mater. 12, 306-313.

Carriba, P., Navarro, G., Ciruela, F., Ferre, S., Casado, V., Agnati, L., Cortes, A., Mallol, J., Fuxe, K., Canela, E.I., Lluis, C., Franco, R., 2008. Nat. Methods 5, 727-733.

Clapp, A.R., Medintz, I.L., Matthew Mauro, J., Fisher, B.R., Bawendi, M.G., Mattoussi, H., 2004. J. Am. Chem. Soc. 126, 301-310.

Derfus, A.M., Chan, W.C., Bhatia, S.N., 2004. Nano Lett. 4, 11-18.

Ding, S.Y., Jones, M., Tucker, M.P., Nedeljkovic, J.M., Wall, J., Simon, M.N., Rumbles, G., Himmel, M.E., 2003. Nano Lett. 3, 1581-1585.

Ding, Z.F., Quinn, B.M., Haram, S.K., Pell, L.E., Korgel, B.A., Bard, A.J., 2002. Science 296, 1293-1297.

Dong, Y.Q., Zhou, N.N., Lin, X.M., Lin, J.P., Chi, Y.W., Chen, G.N., 2010. Chem. Mater. 22, 5895-5899.

Erogbogbo, F., Yong, K.T., Roy, I., Xu, G.X., Prasad, P.N., Swihart, M.T., 2008. ACS Nano 2, 873-878.

Erogbogbo, F., Yong, K.T., Roy, I., Hu, R., Law, W.C., Zhao, W.W., Ding, H., Wu, F., Kumar, R., Swihart, M., Prasad, P.N., 2011. ACS Nano 5, 413-423.

He, Y., Fan, C.H., Lee, S.T., 2010. Nano Today 5, 282-295.

He, Y., Su, Y.Y., Yang, X.B., Kang, Z.H., Xu, T.T., Zhang, R.Q., Fan, C.H., Lee, S.T., 2009. J. Am. Chem. Soc. 131, 4434-4438.

He, Y., Kang, Z.H., Li, Q.S., Tsang, C.H.A., Fan, C.H., Lee, S.T., 2009. Angew. Chem., Int. Ed. 48, 128-132.

He, Y., Kang, Z.H., Li, Q.S., Tsang, C.H.A., Fan, C.H., Lee, S.T., 2009. Angew. Chem. 121, 134-138.

He, Y., Zhong, Y.L., Peng, F., Wei, X.P., Su, Y.Y., Lu, Y.M., Su, S., Gu, W., Liao, L.S., Lee, S.T., 2011. J. Am. Chem. Soc. 133, 14192-14195.

Hou, J., Zhang, H.C., Yang, Q., Li, M.Z., Song, Y.L., Jiang, L., 2014. Angew. Chem., Int. Ed. 53, 5791-5795.

Jennings, T.L., Singh, M.P., Strouse, G.F., 2006. J. Am. Chem. Soc. 128, 5462-5467.

Jiang, Y.L., Wang, Z.Y., Dai, Z.H., 2016. ACS Appl. Mater. Interfaces 8, 3644-3650.

Lee, J.S., Joung, H.A., Kim, M.G., Park, C.B., 2012. ACS Nano 6, 2978-2983.

Li, J., Guo, S.J., Wang, E.K., 2012. RSC Adv. 2, 3579-3586.

Li, M.Z., He, F., Liao, Q., Liu, J., Xu, L., Jiang, L., Song, Y.L., Wang, S., Zhu, D.B., 2008. Angew. Chem., Int. Ed. 47, 7258-7262.

Li, Z.F., Ruckenstein, E., 2004. Nano Lett. 4, 1463-1467.

Liu, S., Tian, J.Q., Wang, L., Zhang, Y.W., Qin, X.Y., Luo, Y.L., Asiri, A.M., Al-Youbi, A.O., Sun, X.P., 2012. Adv. Mater. 24, 2037-2041.

Lu, W.B., Qin, X.Y., Liu, S., Chang, G.H., Zhang, Y.W., Luo, Y.L., Asiri, A.D., Al-Youbi, A.O., Sun, X.P., 2012. Anal. Chem. 84, 5351-5357.

Miao, W.J., 2008. Chem. Rev. 108, 2506-2553.

Michalet, X., Pinaud, F.F., Bentolila, L.A., Tsay, J.M., Doose, S., Li, J.J., Sundaresan, G., Wu, A.M., Gambhir, S.S., Weiss, S., 2005. Science 307, 538-544.

Montalti, M., Cantelli, A., Battistelli, G., 2015. Chem. Soc. Rev. 44, 4853-4921.

Pingarron, J.M., Yanez-Sedeno, P., Gonzalez-Cortes, A., 2008. Electrochim. Acta 53, 5848-5866.

Richter, M.M., 2004. Chem. Rev. 104, 3003-3036.

Sapsford, K.E., Medintz, I.L., Golden, J.P., Deschamps, J.R., Uyeda, H.T., Mattoussi, H., 2004. Langmuir 20, 7720-7728.

Sapsford, K.E., Berti, L., Medintz, I.L., 2006. Angew. Chem. Int. Ed. 45, 4562-4589.

Sham, T.K., Jiang, D.T., Coulthard, I., Lorimer, J.W., Feng, X.H., Tan, K.H., Frigo, S.P., Rosenberg, R.A., Houghton, D.C., Bryskiewicz, B., 1993. Nature 363, 331-334.

Shan, Y., Xu, J.J., Chen, H.Y., 2009. Chem. Commun. 905-907.

Shen, W.Z., Li, M.Z., Wang, B.L., Liu, J., Li, Z.Y., Jiang, L., Song, Y.L., 2012. J. Mater. Chem. 22, 8127-8133.

Shi, L.F., De Paoli, V., Rosenzweig, N., Rosenzweig, Z., 2006. J. Am. Chem. Soc. 128, 10378-10379.

Shiohara, A., Hanada, S., Prabakar, S., Fujioka, K., Lin, T.H., Yamamoto, K., Northcote, P., Tilley, R.D., 2010. J. Am. Chem. Soc. 132, 248-253.

Song, S.P., Qin, Y., He, Y., Huang, Q., Fan, C.H., Chen, H.Y., 2010. Chem. Soc. Rev. 39, 4234-4243.

Sun, Y.P., 2006. J. Am. Chem. Soc. 128, 7756-7757.

Tian, C.Y., Zhao, W.W., Wang, J., Xu, J.J., Chen, H.Y., 2012. Analyst 137, 3070-3075.

Wang, C., Tang, Y., Liu, Y., Guo, Y., 2014. Anal. Chem. 86, 6433-6438.

Wang, D., Rogach, A.L., Caruso, F., 2002. Nano. Lett. 2, 857-861.

Warner, J.H., Hoshino, A., Yamamoto, K., Tilley, R.D., 2005. Angew. Chem., Int. Ed. 44, 4550-4554.

Wilson, W.L., Szajowski, P.F., Brus, L.E., 1993. Science 262, 1242-1244.

Wu, M.S., Shi, H.W., Xu, J.J., Chen, H.Y., 2011. Chem. Commun. 47, 7752-7754.

Wu, M.S., Shi, H.W., He, L.J., Xu, J.J., Chen, H.Y., 2012. Anal. Chem. 84, 4207-4213.

Zheng, L.Y., Chi, Y.W., Dong, Y.Q., Lin, J.P., Wang, B.B., 2009. J. Am. Chem. Soc. 131, 4564-4565.

Zhong, Y.L., Peng, F., Bao, F., Wang, S.Y., Ji, X.Y., Yang, L., Su, Y.Y., Lee, S.T., He, Y., 2013. J. Am. Chem. Soc. 135, 8350-8356.

Zhou, H., Zhang, Y.Y., Liu, J., Xu, J.J., Chen, H.Y., 2012. J. Phys. Chem. C 116, 17773-17780.

Highlights

- Strong cathodic ECL of SiQDs was obtained in neutral condition.
- ECL resonance energy transfer occurred between SiQDs and AuNPs.
- An ECL biosensor was fabricated to sensitively detect DNA.